Ground-State Cooling and High-Fidelity Quantum Transduction via Parametrically Driven Bad-Cavity Optomechanics

Hoi-Kwan Lau* and Aashish A. Clerk
Pritzker School of Molecular Engineering, University of Chicago, 5640 South Ellis Avenue, Chicago, Illinois 60637, USA

(Received 8 May 2019; accepted 20 February 2020; published 10 March 2020)

Optomechanical couplings involve both beam splitter and two-mode-squeezing types of interactions. While the former underlies the utility of many applications, the latter creates unwanted excitations and is usually detrimental. In this Letter, we propose a simple but powerful method based on cavity parametric driving to suppress the unwanted excitation that does not require working with a deeply sideband-resolved cavity. Our approach is based on a simple observation: as both the optomechanical two-mode-squeezing interaction and the cavity parametric drive induce squeezing transformations of the relevant photonic bath modes, they can be made to cancel one another. We illustrate how our method can cool a mechanical oscillator below the quantum backaction limit, and significantly suppress the output noise of a sideband-unresolved optomechanical transducer.

DOI: 10.1103/PhysRevLett.124.103602

Introduction.—Optomechanical systems couple mechanical to electromagnetic degrees of freedom, and have a wide range of utility in both classical and quantum settings [1,2]. Experiments almost always employ a strong electromagnetic drive, with the resulting optomechanical coupling containing both a beam splitter (BS) interaction and a two-mode-squeezing interaction (TMSI). The BS interaction exchanges phononic and photonic excitations, and underlies the functionality of numerous optomechanical applications. This includes cavity cooling of a mechanical mode, where mechanical excitations are transferred to the dissipative electromagnetic cavity [3,4]. It also includes the application of quantum transduction: the mechanical oscillator and BS interaction can be used to mediate microwave to optics quantum state transfer [5–8], which is crucial for distributed quantum information processing [6,9,10].

In these applications, the TMSI, which simultaneously creates both motional and photonic excitations, is highly undesirable. The standard strategy is to partially suppress TMSI by making it highly nonresonant, via an appropriate choice of drive frequency and the use of low-loss cavities whose damping rate κ is much smaller than the mechanical frequency Ω_m. This however places stringent restrictions on experimental platforms. For cavity cooling, the residual TMSI sets the fundamental quantum backaction limit on the lowest achievable mechanical occupancy [11,12]. This limit prevents approaching the quantum ground state for sideband unresolved systems having $\kappa \gtrsim \Omega_m$. Strategies for ground state cooling have been formulated for the latter systems (e.g., dissipative coupling [13–16], coupling to trapped atoms [17–19], photonic squeezing [20–23]); however, they present their own implementation challenges. Similarly, TMSI makes high fidelity quantum transduction impossible in the sideband unresolved systems, and even constrains the performance of sideband resolved systems [7,8]. Therefore, sideband-resolving cavity is widely believed to be necessary for efficient transduction [9], and we are not aware of any correction strategy.

In this Letter, we propose simple but powerful strategies to suppress the deleterious effects in sideband-unresolved optomechanics applications. Our strategy is based on two key observations. First, unwanted backaction effect arises because the mechanical oscillator is driven by electromagnetic vacuum noise that is squeezed by the TMSI. Second, parametric (i.e., two-photon) driving induces additional electromagnetic squeezing, so that the net squeezing of the cavity backaction can be minimized by optimizing system parameters. Remarkably, our strategy can completely eliminate TMSI imperfections in sideband unresolved systems in the typical operation regime of large cooperativity but no strong coupling. In the case of cooling, our strategy completely eliminates backaction heating. In the case of transduction, parametric drive removes the unwanted amplification of the input signal. With this improvement, we are also able to obtain a new impedance-matching condition and injected squeezing strategy, which both improve the transmission bandwidth and suppress the added noise of the output signal.

Parametrically driven optomechanics.—We consider a generic optomechanical system where two cavities ($\hat{a}_1$ and $\hat{a}_2$) are coupled to the same mechanical oscillator ($\hat{a}_m$) [see Fig. 1(a)]; each cavity is subject to both a linear drive and a parametric drive (PD), and the drive frequencies for each cavity are commensurate. After making standard displacement and linearization transformations [2], the mode dynamics obey the Langevin equations

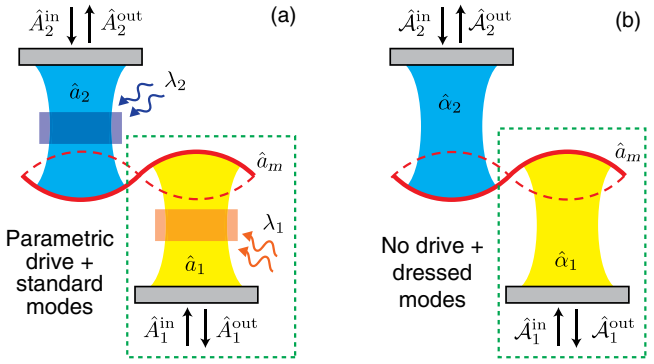

FIG. 1. (a) Generic optomechanical system described by Eq. (1), where two parametrically driven cavities ($\hat{a}_1$, $\hat{a}_2$) couple to a common mechanical oscillator ($\hat{a}_m$). (b) An equivalent optomechanical system described by Eq. (3), which is not parametrically driven but where both the bath and cavity modes are squeezed. Both cavity modes 1 and 2 are involved in transduction, but only cavity mode 1 is utilized in cooling (inside green dotted box).

$$\dot{\hat{a}}_i = -i\left(\Delta_i - i\frac{\kappa_i}{2}\right)\hat{a}_i - i\lambda_i\hat{a}_i^\dagger - iG_i(\hat{a}_m + \hat{a}_m^\dagger) - i\sqrt{\kappa_i}\hat{A}_i^{\mathrm{in}},$$
$$\dot{\hat{a}}_m = -i\left(\Omega_m - i\frac{\gamma}{2}\right)\hat{a}_m - i\sum_{i=1,2} G_i(\hat{a}_i + \hat{a}_i^\dagger) - i\sqrt{\gamma}\hat{A}_m^{\mathrm{in}}, \qquad (1)$$

or in a compact form $\dot{\vec{a}} = -i\boldsymbol{H}\vec{a} + \boldsymbol{K}\vec{A}^{\mathrm{in}}$, where we index vectors and matrices according to the mode operators, i.e., for any vector $\vec{v} \equiv (v_1, v_{1^\dagger}, v_m, v_{m^\dagger}, v_2, v_{2^\dagger})^T$, and similarly for matrices; $\boldsymbol{K} \equiv \mathrm{diag}(-i\sqrt{\kappa_1}, i\sqrt{\kappa_1}, -i\sqrt{\gamma}, i\sqrt{\gamma}, -i\sqrt{\kappa_2}, i\sqrt{\kappa_2})$. $\hat{A}_i^{\mathrm{in}}$ and $\hat{A}_m^{\mathrm{in}}$, respectively, describe the incident noise on cavity i and the mechanical oscillator; we take $\hat{A}_i^{\mathrm{in}}$ to correspond to vacuum noise unless specified otherwise. The dynamical matrix $\boldsymbol{H}$ contains all system parameters: $\Delta_i, \lambda_i, \kappa_i$, and G_i are the mode-drive frequency detuning, PD strength, dissipation rate, and many-photon optomechanical coupling strength of cavity i; Ω_m and γ are the frequency and damping rate of mechanical oscillator.

We focus attention on parameters where the detunings are large enough that the system is dynamically stable when $G_i = 0$ and even without dissipation, i.e., $|\lambda_i| < |\Delta_i|$. More discussion about the general system stability is given in Supplemental Material [24]. The Hamiltonian of each isolated (but parametrically driven) cavity can be diagonalized in terms of a dressed (Bogoliubov) mode: $\hat{\alpha}_i = e^{i\phi_i}\cosh r_i \hat{a}_i + e^{i\phi_i}e^{i\theta_i}\sinh r_i \hat{a}_i^\dagger$, for $i \in \{1, 2\}$. The transformation parameters are

$$e^{i\theta_i}\tanh 2r_i \equiv \lambda_i/\Delta_i, \qquad e^{i\phi_i} \equiv \mu_i/|\mu_i|, \qquad (2)$$

where $\mu_i \equiv \cosh r_i - e^{i\theta_i}\sinh r_i$. The evolution of the dressed modes follow

$$\dot{\hat{\alpha}}_i = -i\left(\tilde{\Delta}_i - i\frac{\kappa_i}{2}\right)\hat{\alpha}_i - i\mathcal{G}_i(\hat{a}_m + \hat{a}_m^\dagger) - i\sqrt{\kappa_i}\hat{\mathcal{A}}_i^{\mathrm{in}},$$
$$\dot{\hat{a}}_m = -i\left(\Omega_m - i\frac{\gamma}{2}\right)\hat{a}_m - i\sum_{i=1,2}\mathcal{G}_i(\hat{\alpha}_i + \hat{\alpha}_i^\dagger) - i\sqrt{\gamma}\hat{A}_m^{\mathrm{in}}, \qquad (3)$$

or in the compact form $\dot{\vec{\alpha}} = -i\mathcal{H}\vec{\alpha} + \boldsymbol{K}\vec{\mathcal{A}}^{\mathrm{in}}$ [30]. The dressed modes have modified detunings and optomechanical coupling as $\tilde{\Delta}_i \equiv \sqrt{\Delta_i^2 - |\lambda_i|^2} > 0$ and $\mathcal{G}_i \equiv |\mu_i| G_i$, but their dissipation rates remain κ_i. Hereafter, we implicitly assume weak coupling and low mechanical dampling, i.e., $\gamma \ll \mathcal{G}_1, \mathcal{G}_2 \ll \tilde{\Delta}_i, \kappa_i$, which is the typical experimental regime.

The noise-free dynamics of the dressed modes in Eq. (3) corresponds to a standard optomechanical system with no PD. This structure results from the optomechanical coupling being a product of quadratures, a structure that is preserved after a Bogoliubov transformation [31]. The main difference in Eq. (3) is in the noise terms: the input noise from the cavity baths now appears squeezed:

$$\hat{\mathcal{A}}_i^{\mathrm{in}} \equiv e^{i\phi_i}\cosh r_i \hat{A}_i^{\mathrm{in}} - e^{i\phi_i}e^{i\theta_i}\sinh r_i \hat{A}_i^{\mathrm{in}\dagger}. \qquad (4)$$

Hence, the PDs have allowed us to map our system (which is driven by vacuum noise) to a standard optomechanical system driven by squeezed noise.

As we will see, TMSI is detrimental because it induces unwanted squeezing of the bath fluctuations; this squeezing is large when $\kappa \gtrsim \Omega_m$. To correct such effects, our systematic strategy is to use PD to counteract this squeezing. We first determine the PD parameters needed for this compensation [cf. Eq. (4)] while keeping the dressed-mode dynamics (as given by $\mathcal{H}$) fixed. Next, we optimize $\mathcal{H}$ for a specific application. Finally, the experimentally relevant "bare" system parameters (given by $\boldsymbol{H}$) can be inferred.

Optomechanical cooling.—We first apply our strategy to suppress the TMSI-induced backaction heating in optomechanical cooling. We consider the standard cooling setup involving only one cavity, and thus decouple cavity 2 by setting $G_2 = 0$. The mechanical steady state is determined by its response to the various input noise operators [11]: $\hat{a}_m[\omega] = \hat{\mathbb{A}}_1(\omega) + \hat{\mathbb{A}}_m(\omega)$, where $\hat{O}[\omega] \equiv \int \hat{O}(t)e^{i\omega t}dt$. $\hat{\mathbb{A}}_1(\omega)$ $[\hat{\mathbb{A}}_m(\omega)]$ contains only the photonic (mechanical) bath operators, and thus corresponds to the backaction (thermal) heating.

Our focus is on the backaction part. In the typical experimental regime of weak coupling and low mechanical damping, the oscillator is mainly influenced by resonant bath modes, i.e., $\omega \approx \Omega_m$. Near this frequency, the backaction heating is determined by a squeezed version of the input noise in Eq. (4):

$$\hat{\mathbb{A}}_1(\omega) \propto e^{i\phi_s(\omega)}\cosh r_s(\omega)\hat{\mathcal{A}}_1^{\mathrm{in}}[\omega] + e^{i\phi_s(\omega)}e^{i\theta_s(\omega)}\sinh r_s(\omega)\hat{\mathcal{A}}_1^{\mathrm{in}\dagger}[\omega]. \qquad (5)$$

The effective squeezing parameters are $e^{i\phi_s(\omega)}\cosh r_s(\omega) \equiv \mathcal{X}_{m,1}(\omega)/\sqrt{|\mathcal{X}_{m,1}(\omega)|^2 - |\mathcal{X}_{m,1^\dagger}(\omega)|^2}$, $e^{i\theta_s(\omega)}\tanh r_s(\omega) \equiv \mathcal{X}_{m,1^\dagger}(\omega)/\mathcal{X}_{m,1}(\omega)$; $\boldsymbol{\mathcal{X}}(\omega) \equiv i(\omega \boldsymbol{I}_6 - \boldsymbol{\mathcal{H}})^{-1}\boldsymbol{K}$ is the susceptibility matrix of the dressed modes; $\boldsymbol{I}_k$ is the $k \times k$ identity.

This picture explains that standard optomechanical cooling suffers from backaction heating because the mechanical oscillator is experiencing a photonic bath that is squeezed by the unwanted TMSI. Our strategy is then to tune the PD so that the $\hat{\mathcal{A}}_1^{\rm in}$ in Eq. (4) is *already* squeezed vacuum noise, such that the additional squeezing in Eq. (5) results in a simple vacuum noise in the vicinity of $\omega \approx \Omega_m$. This requires tuning $2\phi_1 + \theta_1 = \theta_s(\Omega_m)$, and $r_1 = r_s(\Omega_m)$, so the dominant bath mode reduces to vacuum noise:

$$\hat{\mathbb{A}}_1(\Omega_m) \propto \hat{A}_1^{\rm in}[\Omega_m]; \tag{6}$$

this can be satisfied if the parameters follow [24]

$$\lambda_1 = \Delta_1 - \Omega_m - i\kappa_1/2. \tag{7}$$

We note that although previous work provided numerical evidence that parametric driving could be beneficial [20,21], our analysis provides a physically transparent and rigorous understanding of TMSI-induced backaction. This understanding allows us to optimize the system parameters in Eq. (7), which completely eliminates backaction heating and thus allows cavity cooling to the ground state in the deep sideband-unresolved regime.

Typical performance of our strategy is shown in Fig. 2(a), where the backaction excitation, N_{ba}, is suppressed far below the quantum backaction limit in both the sideband

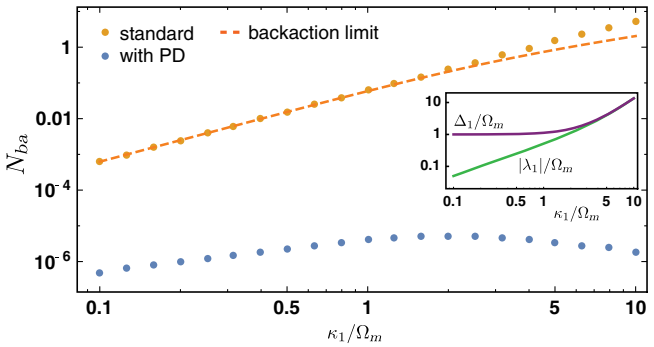

FIG. 2. Cavity backaction heating of the mechanics as a number of quanta $N_{ba} = (1/2\pi)\int\langle\hat{\mathbb{A}}_1^\dagger(\omega)\hat{\mathbb{A}}_1(\omega')\rangle d\omega d\omega'$, versus sideband resolution parameter κ_1/Ω_m. $\tilde{\Delta} = \Omega_m$, $\gamma = 10^{-5}\Omega_m$, and $\mathcal{G}_1$ is tuned to keep the cooperativity as $\mathcal{G}_1^2/\kappa_1\gamma = 10$. At each value of κ_1, the standard (orange) and PD systems (blue) share the same $\boldsymbol{\mathcal{H}}$. Optimal PD reduces N_{ba} to below quantum backaction limit (dashed) $[\sqrt{1 + (\kappa_1/2\Omega_m)^2} - 1]/2$ [11,12]. The remaining excitation is due to nonvanishing but narrow mechanical linewidth ($\sim\mathcal{G}_1^2/\kappa_1$) [24]. (Inset) Cavity mode detuning Δ_1 and PD strength $|\lambda_1|$ for producing the same $\boldsymbol{\mathcal{H}}$.

resolved ($\kappa_1 \ll \Omega_m$) and unresolved ($\kappa_1 \gtrsim \Omega_m$) regimes. We note that our PD strategy does not affect the heating of the mechanics by its intrinsic bath, nor requires increasing optomechanical coupling [24].

Finally, our theory also provides a simple explanation of the injected squeezing (IS) strategy for sideband-unresolved cooling [22,23]. At first glance, both strategies are not obviously related: while the IS strategy requires arbitrarily strong squeezing in the bad cavity limit, the stationary intracavity squeezing generated in our PD approach is bounded by 3 dB [32]. Despite this crucial difference, these strategies are connected: while we use PD to counteract the bath squeezing produced by TMSI, the IS strategy simply injects appropriately squeezed noise into the cavity to get the same kind of cancellation. Explicitly, the goal is $\langle\hat{\mathbb{A}}_1^\dagger(\omega)\hat{\mathbb{A}}_1(\Omega_m)\rangle = 0$, but now in Eq. (5), $\hat{\mathcal{A}}_1^{\rm in}[\omega]$ represents vacuum noise, and $r_s(\omega)$ and $\theta_s(\omega)$ characterize the externally produced squeezing. Using this to determine optimal values of the squeezing parameters reduces to the same conditions found (via a slightly different argument) in Refs. [22,24]. When comparing with the IS strategy, our approach has a crucial practical advantage: it does not require one to externally produce and then transfer with high-fidelity a highly squeezed vacuum state. This avoids the extra thermal noise induced due to transfer loss, which is a major limitating factor of the IS strategy [22,23]. Nevertheless, these two strategies are complementary: the PD strength needed for perfect backaction suppression can be reduced if the photonic input noise is weakly squeezed.

Quantum transduction.—Optomechanical quantum transduction is of enormous interest [5–8]. It requires coupling two cavities (one microwave, one optical) to a common mechanical oscillator, i.e., our setup described in Eq. (1). We take the photonic baths to correspond to coupling waveguides, and take system 1 (2) to be the transducer input (output). The transduction is characterized by the scattering of frequency modes $\vec{A}^{\rm out}[\omega] = \vec{A}^{\rm in}[\omega] + \boldsymbol{K}\vec{a}[\omega] = \boldsymbol{T}(\omega)\vec{A}^{\rm in}[\omega]$, where $\boldsymbol{T}(\omega) \equiv \boldsymbol{I}_6 + i\boldsymbol{K}(\omega\boldsymbol{I}_6 - \boldsymbol{H})^{-1}\boldsymbol{K}$ is the scattering matrix. An ideal transducer requires a frequency mode to be completely transferred, i.e., $\hat{A}_2^{\rm out}[\omega_0] = \hat{A}_1^{\rm in}[\omega_0]$ at an optimal frequency ω_0. In practice, such a condition is usually not satisfied at any ω due to system imperfections.

To focus on the imperfection due to TMSI, we neglect the mechanical loss (i.e., $\gamma \to 0$). The general transformation of a frequency mode is

$$\hat{A}_2^{\rm out}[\omega] = T_{2,1}(\omega)\hat{A}_1^{\rm in}[\omega] + \hat{\mathcal{J}}(\omega), \tag{8}$$

where $\hat{\mathcal{J}}(\omega) \equiv \hat{\mathcal{J}}_T(\omega) + \hat{\mathcal{J}}_R(\omega)$ contains all the unwanted components being mixed into the transmitted mode by TMSI: $\hat{\mathcal{J}}_T(\omega) \equiv T_{2,1^\dagger}(\omega)\hat{A}_1^{\rm in\dagger}[\omega]$ is introduced by the unwanted squeezing of the input, and the unwanted reflection is represented by $\hat{\mathcal{J}}_R(\omega) \equiv T_{2,2}(\omega)\hat{A}_2^{\rm in}[\omega] + T_{2,2^\dagger}(\omega)\hat{A}_2^{\rm in\dagger}[\omega]$.

In analogy to a linear amplifier, the performance of a bosonic transducer can be quantified by its added noise spectral density, i.e., how much extraneous noise is added to the output state [33]

$$2\pi\eta(\omega)S(\omega)\delta(\omega-\omega') \equiv \frac{1}{2}\langle\{\hat{J}(\omega),\hat{J}^{\dagger}(\omega')\}\rangle, \quad (9)$$

where $\eta(\omega)\equiv|T_{2,1}(\omega)|^2$ is the conversion efficiency. For uncorrelated baths 1 and 2, their bosonic properties set a fundamental lower-bound on the added noise [24]:

$$S(\omega) \geq \frac{\mathcal{R}(\omega)}{2} + \left|\frac{1-\eta(\omega)}{2\eta(\omega)} + \frac{\mathcal{R}(\omega)}{2}\right|. \quad (10)$$

Noiseless transduction thus requires a unit conversion efficiency, $\eta(\omega)\to 1$, and a vanishing conjugated transmission (i.e., amplification), $\mathcal{R}(\omega)\equiv|T_{2,1^{\dagger}}(\omega)|^2/|T_{2,1}(\omega)|^2\to 0$, at an optimal frequency $\omega\to\omega_0$.

These conditions are generally not satisfied at any ω for sideband unresolved optomechanical transducers, however we here show that they can be systematically achieved by parametrically driving only the input cavity $\hat{a}_1$, and injecting squeezing to (but not parametrically driving) the output cavity $\hat{a}_2$. Our strategy again consists of tuning the PD and system parameters in such a way that the dressed-mode dynamical matrix $\boldsymbol{\mathcal{H}}$ [and hence dressed-mode scattering matrix $\boldsymbol{\mathcal{T}}(\omega)\equiv\boldsymbol{I}_6+\boldsymbol{K}\boldsymbol{\mathcal{X}}(\omega)$] remains unchanged. The relation between the dressed-mode and original-mode scattering matrices is

$$\vec{A}^{\text{out}}[\omega] = \boldsymbol{T}(\omega)\vec{A}^{\text{in}}[\omega] = \boldsymbol{\mathcal{F}}^{-1}\boldsymbol{\mathcal{T}}(\omega)\boldsymbol{\mathcal{F}}\vec{A}^{\text{in}}[\omega], \quad (11)$$

where the PD-induced squeezing is described by $\boldsymbol{\mathcal{F}}_1\equiv\begin{pmatrix} e^{i\phi_i}\cosh r_1 & -e^{i\phi_1}e^{i\theta_1}\sinh r_1 \\ -e^{-i\phi_1}e^{-i\theta_1}\sinh r_1 & e^{-i\phi_1}\cosh r_1\end{pmatrix}$ and $\boldsymbol{\mathcal{F}}\equiv\text{diag}(\boldsymbol{\mathcal{F}}_1,\boldsymbol{I}_4)$. For simplicity, we assume all dressed modes are resonant, i.e., $\tilde{\Delta}_1=\tilde{\Delta}_2=\Omega_m$, although a generalization beyond this regime is straightforward.

To correct the unwanted amplification [i.e., $\mathcal{R}(\omega)\neq 0$], we first consider the transmission block of the scattering matrix in Eq. (11), which gives $T_{2,1^{\dagger}}(\omega)=e^{-i\phi_1}\cosh r_1\mathcal{T}_{2,1^{\dagger}}(\omega)-e^{i\phi_1}e^{i\theta_1}\sinh r_1\mathcal{T}_{2,1}(\omega)$. At any specific ω, the TMSI-induced amplification can be corrected by a PD-induced squeezing, such that $T_{2,1^{\dagger}}(\omega)=0$. The required squeezing parameters follow

$$e^{i2\phi_1}e^{i\theta_1}\tanh r_1 = \mathcal{T}_{2,1^{\dagger}}(\omega)/\mathcal{T}_{2,1}(\omega). \quad (12)$$

Apart from correcting unwanted amplification by PD, we also need to choose the system parameters that yield unity conversion efficiency $\eta(\omega)=1$. From the detailed expression of conversion efficiency [24], we find that it is maximized when $\Gamma_1=\Gamma_2$, where

$$\Gamma_i \equiv \frac{4\mathcal{G}_i^2}{\kappa_i} - \frac{(\kappa_i/4\Omega_m)^2}{1+(\kappa_i/4\Omega_m)^2}\frac{4\mathcal{G}_i^2}{\kappa_i}. \quad (13)$$

Γ_i is nothing but the net optical damping rate of the mechanics due to cavity; the condition $\Gamma_1=\Gamma_2$ can thus be seen as a generalized impedance matching condition.

Because of the TMSI-induced amplification, the peak efficiency will in general be higher than unity [$\max(\eta)>1$], which prevents optimizing the added noise. To optimize this added noise over a reasonable bandwidth, it is thus desirable to *deliberately* impedance mismatch the system so that $\max(\eta)=1$. This requires satisfying the modified impedance matching condition [24]:

$$\left(1+\left(\frac{\kappa_2}{4\Omega_m}\right)^2\right)\left(\frac{\sqrt{\Gamma_1\Gamma_2}}{(\Gamma_1+\Gamma_2)/2}\right)^2 = 1. \quad (14)$$

With this choice, the conversion efficiency is close to unity for the frequency modes around $\omega_0=\Omega_m-(\kappa_1\Gamma_1+\kappa_2\Gamma_2)/8\Omega_m$.

Finally, achieving the lower bound in Eq. (10) also requires optimizing the input noise injected into the *output* of our transducer (i.e., $\hat{a}_2$). At the optimal frequency where $\eta(\omega_0)=1$ and $\mathcal{R}(\omega_0)=0$ (hence $\hat{J}_T(\omega_0)=0$), the added noise only involves the cavity-2 bath, via the operator $\hat{J}_R(\omega_0)$. We find that the commutation relation of Eq. (8) imposes $|T_{2,2}(\omega_0)|=|T_{2,2^{\dagger}}(\omega_0)|$, which requires the real and imaginary parts of $\hat{J}_R(\omega_0)$ to be two distinct but *commuting* quadrature operators. As such, the added noise can be suppressed by injecting to cavity-2 a bath that is squeezed in both of these quadratures. In practice, this squeezing is achievable by having broadband single-mode squeezing. Explicitly, we consider a squeezed bath with correlations $\langle\hat{A}_2^{\text{in}\dagger}(t)\hat{A}_2^{\text{in}}(t')\rangle=\delta(t-t')\sinh^2 s$ and $\langle\hat{A}_2^{\text{in}}(t)\hat{A}_2^{\text{in}}(t')\rangle=\delta(t-t')e^{i\vartheta}\sinh s\cosh s$. By evaluating Eq. (9), the added noise at $\omega=\omega_0$ is suppressed for increasing squeezing strength s: $S(\omega_0)=e^{-2s}|T_{2,2^{\dagger}}(\omega_0)|^2$ when the squeezing phase is optimized as $e^{i\vartheta}=-T_{2,2^{\dagger}}(\omega_0)/T_{2,2}(\omega_0)$.

The performance of a typical optomechanical transducer that is only weakly sideband resolved is shown in Fig. 3. As shown, our approach gives a marked improvement in the transduction fidelity. We note that even when there is mechanical loss, $\gamma\neq 0$, our PD strategy would not amplify the additional contribution to the transducer added noise coming from the intrinsic mechanical bath. This is because such noise is determined by the scattering amplitudes $T_{2,m}(\omega)$ and $T_{2,m^{\dagger}}(\omega)$, which is unaltered if the system parameters are tuned to preserve $\boldsymbol{\mathcal{H}}$ [cf. Eq. (11)].

Our strategy can improve the performance of microwave-optics transducer, which is a crucial component in a superconducting quantum computer network [5]. For microwave-to-optics transfer, our strategy requires a microwave-cavity PD and injected optical squeezing, which both

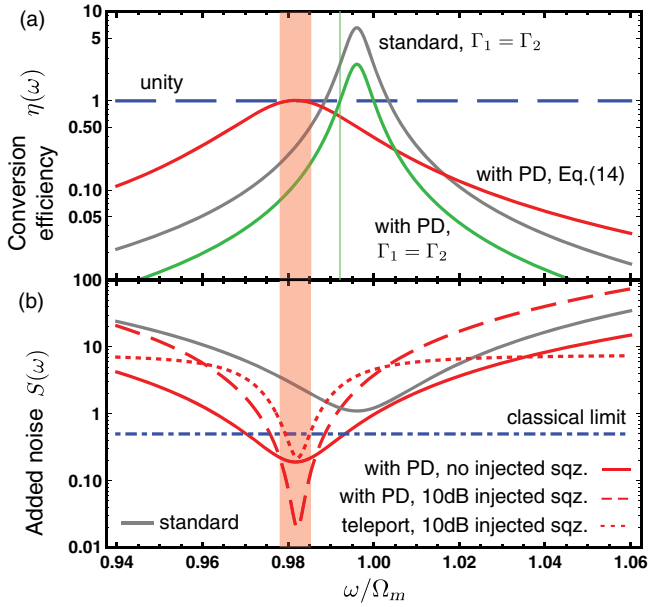

FIG. 3. (a) Conversion efficiency $\eta(\omega)$ of optomechanical transducers with $\tilde{\Delta}_1 = \tilde{\Delta}_2 = \Omega_m$, $\kappa_1 = \kappa_2 = 5\Omega_m$, and $\mathcal{G}_2 = 0.1\Omega_m$. (Grey) standard transducer: no PD and $\Gamma_1 = \Gamma_2$. (Green) optimal PD in (12) with $\Gamma_1 = \Gamma_2$. (Red) our strategy: optimal PD and modified impedance matching in Eq. (14). Transduction windows with $|1 - \eta(\omega)| < 5\%$ are shown for the PD systems. Modified impedance matching (red shaded) yields a much wider bandwidth than picking $\Gamma_1 = \Gamma_2$ (green shaded). (b) Added noise $S(\omega)$ for the transducers. (Dot dashed) $S(\omega) = 0.5$, above which more noise is added in coherent state transduction than classical cloning [34,35]. (Grey) standard transducer adds more noise than the classical limit in this scenario, i.e., no quantum transduction. Our strategy can yield a transduction with lower noise even when the bath is vacuum (red solid); the noise can further be suppressed by injecting 10 dB squeezing (red dashed). (Red dotted) teleportation strategy with 10 dB input two-mode squeezing and 10 dB injected squeezing at output port.

have been realized with high quality [36–39]. For the reverse direction (i.e., optics-to-microwave), an optical-cavity PD is instead required. With numerous exciting prospects [40–43], optical-cavity PD has been experimentally implemented by embedding nonlinear crystals in optical cavities [39,44,45] or fabricating microcavities with nonlinear materials [38,46].

Alternatively, one can apply our strategy for optics-to-microwave transfer *without* any need for an optical-cavity PD by combining it with quantum teleportation [34,47] (more details and schematic illustration are given in Supplemental Material [24]). One first prepares a microwave two-mode-squeezed state, injecting one half into a microwave-to-optics transducer, emerging at the output of the optical cavity. The input optical state to be transduced is not injected into the transducer; instead, one makes a continuous-variable Bell measurement on this state and the optical-cavity output state. After feed forward, the original optical input state can be recovered from the remaining half of the microwave two-mode-squeezed state. This method replaces the technically challenging optical parametric drive by highly efficient microwave squeezing [48–51] and optical homodyne detection [52].

Conclusion.—In this work we study the backaction effects of TMSI in sideband unresolved optomechanical systems. We show that most detrimental effects originate from the squeezing of photonic bath, which can be corrected by a controlled squeezing through parametrically driving the photonic cavity. We show explicitly how our strategy can eliminate backaction heating in optomechanical cooling, and correct unwanted amplification in quantum transduction. Although our analysis is focused on optomechanical systems, the technique is also applicable to eliminate TMSI-induced unwanted effects in other hybrid quantum platforms, such as electro-optical [53–55] and magnomechanical systems [56].

This work is supported by the AFOSR MURI FA9550-15-1-0029 on quantum transduction, and the DARPA DRINQS program (Agreement No. D18AC00014).

Note added.—Recently, we became aware of the appearance of related articles, Refs. [57,58], which also discuss improved optomechanical cooling with parametric drive. However, these works do not consider the application of parametric drive in quantum transduction.

*hklau.physics@gmail.com

[1] C. K. Law, Phys. Rev. A **51**, 2537 (1995).
[2] M. Aspelmeyer, T. J. Kippenberg, and F. Marquardt, Rev. Mod. Phys. **86**, 1391 (2014).
[3] J. D. Teufel, T. Donner, D. Li, J. W. Harlow, M. S. Allman, K. Cicak, A. J. Sirois, J. D. Whittaker, K. W. Lehnert, and R. W. Simmonds, Nature (London) **475**, 359 (2011).
[4] J. Chan, T. P. M. Alegre, A. H. Safavi-Naeini, J. T. Hill, A. Krause, S. Gröblacher, M. Aspelmeyer, and O. Painter, Nature (London) **478**, 89 (2011).
[5] A. H. Safavi-Naeini and O. Painter, New J. Phys. **13**, 013017 (2011).
[6] C. A. Regal and K. W. Lehnert, J. Phys. Conf. Ser. **264**, 012025 (2011).
[7] R. W. Andrews, R. W. Peterson, T. P. Purdy, K. Cicak, R. W. Simmonds, C. A. Regal, and K. W. Lehnert, Nat. Phys. **10**, 321 (2014).
[8] A. P. Higginbotham, P. S. Burns, M. D. Urmey, R. W. Peterson, N. S. Kampel, B. M. Brubaker, G. Smith, K. W. Lehnert, and C. A. Regal, Nat. Phys. **14**, 1038 (2018).
[9] L. Tian, Ann. Phys. (Amsterdam) **527**, 1 (2015).
[10] G. Kurizki, P. Bertet, Y. Kubo, K. Molmer, D. Petrosyan, P. Rabl, and J. Schmiedmayer, Proc. Natl. Aacd. Sci. U.S.A. **112**, 3866 (2015).
[11] F. Marquardt, J. P. Chen, A. A. Clerk, and S. M. Girvin, Phys. Rev. Lett. **99**, 093902 (2007).
[12] I. Wilson-Rae, N. Nooshi, W. Zwerger, and T. J. Kippenberg, Phys. Rev. Lett. **99**, 093901 (2007).

[13] F. Elste, S. M. Girvin, and A. A. Clerk, Phys. Rev. Lett. **102**, 207209 (2009).
[14] A. Xuereb, R. Schnabel, and K. Hammerer, Phys. Rev. Lett. **107**, 213604 (2011).
[15] A. Sawadsky, H. Kaufer, R. M. Nia, S. P. Tarabrin, F. Y. Khalili, K. Hammerer, and R. Schnabel, Phys. Rev. Lett. **114**, 043601 (2015).
[16] S. Huang and A. Chen, Phys. Rev. A **98**, 063818 (2018).
[17] C. Genes, H. Ritsch, and D. Vitali, Phys. Rev. A **80**, 061803(R) (2009).
[18] C. Genes, H. Ritsch, M. Drewsen, and A. Dantan, Phys. Rev. A **84**, 051801(R) (2011).
[19] H.-K. Lau, A. Eisfeld, and J.-M. Rost, Phys. Rev. A **98**, 043827 (2018).
[20] S. Huang and G. S. Agarwal, Phys. Rev. A **79**, 013821 (2009).
[21] A. Asghari Nejad, H. R. Askari, and H. R. Baghshahi, Physica (Amsterdam) **102E**, 83 (2018).
[22] J. B. Clark, F. Lecocq, R. W. Simmonds, J. Aumentado, and J. D. Teufel, Nature (London) **541**, 191 (2017).
[23] M. Asjad, S. Zippilli, and D. Vitali, Phys. Rev. A **94**, 051801 (R) (2016).
[24] See the Supplemental Material at http://link.aps.org/supplemental/10.1103/PhysRevLett.124.103602 for more details, which also contains Refs. [25–29].
[25] Y.-D. Wang, S. Chesi, and A. A. Clerk, Phys. Rev. A **91**, 013807 (2015).
[26] E. X. DeJesus and C. Kaufman, Phys. Rev. A **35**, 5288 (1987).
[27] G. A. Peterson, S. Kotler, F. Lecocq, K. Cicak, X. Y. Jin, R. W. Simmonds, J. Aumentado, and J. D. Teufel, Phys. Rev. Lett. **123**, 247701 (2019).
[28] R. Filip, Phys. Rev. A **80**, 022304 (2009).
[29] M. Zhang, C.-L. Zou, and L. Jiang, Phys. Rev. Lett. **120**, 020502 (2018).
[30] Note that the mechanical mode and bath are unaffected by the diagonalization, i.e., $\hat{\alpha}_m = \hat{a}_m$ and $\hat{\mathcal{A}}_m^{\mathrm{in}} = \hat{A}_m^{\mathrm{in}}$.
[31] C. Weedbrook, S. Pirandola, R. García-Patrón, N. J. Cerf, T. C. Ralph, J. H. Shapiro, and S. Lloyd, Rev. Mod. Phys. **84**, 621 (2012).
[32] G. Milburn and D. F. Walls, Opt. Commun. **39**, 401 (1981).
[33] C. M. Caves, Phys. Rev. D **26**, 1817 (1982).
[34] S. L. Braunstein and P. van Loock, Rev. Mod. Phys. **77**, 513 (2005).
[35] H.-K. Lau and A. A. Clerk, npj Quantum Inf. **5**, 31 (2019).
[36] T. Yamamoto, K. Inomata, M. Watanabe, K. Matsuba, T. Miyazaki, W. D. Oliver, Y. Nakamura, and J. S. Tsai, Appl. Phys. Lett. **93**, 042510 (2008).
[37] M. A. Castellanos-Beltran, K. D. Irwin, G. C. Hilton, L. R. Vale, and K. W. Lehnert, Nat. Phys. **4**, 929 (2008).
[38] J. U. Fürst, D. V. Strekalov, D. Elser, A. Aiello, U. L. Andersen, C. Marquardt, and G. Leuchs, Phys. Rev. Lett. **106**, 113901 (2011).
[39] H. Vahlbruch, M. Mehmet, K. Danzmann, and R. Schnabel, Phys. Rev. Lett. **117**, 110801 (2016).
[40] V. Peano, H. G. L. Schwefel, C. Marquardt, and F. Marquardt, Phys. Rev. Lett. **115**, 243603 (2015).
[41] X.-Y. Lü, Y. Wu, J. R. Johansson, H. Jing, J. Zhang, and F. Nori, Phys. Rev. Lett. **114**, 093602 (2015).
[42] C. Leroux, L. C. G. Govia, and A. A. Clerk, Phys. Rev. Lett. **120**, 093602 (2018).
[43] W. Qin, A. Miranowicz, P.-B. Li, X.-Y. Lü, J. Q. You, and F. Nori, Phys. Rev. Lett. **120**, 093601 (2018).
[44] H. Vahlbruch, M. Mehmet, S. Chelkowski, B. Hage, A. Franzen, N. Lastzka, S. Goßler, K. Danzmann, and R. Schnabel, Phys. Rev. Lett. **100**, 033602 (2008).
[45] R. Schnabel, Phys. Rep. **684**, 1 (2017).
[46] M. Förtsch, J. U. Fürst, C. Wittmann, D. Strekalov, A. Aiello, M. V. Chekhova, C. Silberhorn, G. Leuchs, and C. Marquardt, Nat. Commun. **4**, 1818 (2013).
[47] S. Pirandola, J. Eisert, C. Weedbrook, A. Furusawa, and S. L. Braunstein, Nat. Photonics **9**, 641 (2015).
[48] E. P. Menzel, R. Di Candia, F. Deppe, P. Eder, L. Zhong, M. Ihmig, M. Haeberlein, A. Baust, E. Hoffmann, D. Ballester, K. Inomata, T. Yamamoto, Y. Nakamura, E. Solano, A. Marx, and R. Gross, Phys. Rev. Lett. **109**, 250502 (2012).
[49] C. Eichler, Y. Salathé, J. Mlynek, S. Schmidt, and A. Wallraff, Phys. Rev. Lett. **113**, 110502 (2014).
[50] K. G. Fedorov, L. Zhong, S. Pogorzalek, P. Eder, M. Fischer, J. Goetz, E. Xie, F. Wulschner, K. Inomata, T. Yamamoto, Y. Nakamura, R. Di Candia, U. Las Heras, M. Sanz, E. Solano, E. P. Menzel, F. Deppe, A. Marx, and R. Gross, Phys. Rev. Lett. **117**, 020502 (2016).
[51] A. Bienfait, P. Campagne-Ibarcq, A. H. Kiilerich, X. Zhou, S. Probst, J. J. Pla, T. Schenkel, D. Vion, D. Esteve, J. J. L. Morton, K. Moelmer, and P. Bertet, Phys. Rev. X **7**, 041011 (2017).
[52] M. Fuwa, S. Takeda, M. Zwierz, H. M. Wiseman, and A. Furusawa, Nat. Commun. **6**, 6665 (2015).
[53] M. Tsang, Phys. Rev. A **81**, 063837 (2010).
[54] M. Tsang, Phys. Rev. A **84**, 043845 (2011).
[55] A. Rueda, F. Sedlmeir, M. C. Collodo, U. Vogl, B. Stiller, G. Schunk, D. V. Strekalov, C. Marquardt, J. M. Fink, O. Painter, G. Leuchs, and H. G. L. Schwefel, Optica **3**, 597 (2016).
[56] X. Zhang, C.-L. Zou, L. Jiang, and H. X. Tang, Sci. Adv. **2**, e1501286 (2016).
[57] M. Asjad, N. E. Abari, S. Zippilli, and D. Vitali, Opt. Express **27**, 32427 (2019).
[58] J. H. Gan, Y. C. Liu, C. Lu, X. Wang, M. K. Tey, and L. You, Laser Photonics Rev. **13**, 1900120 (2019).